

Biomechanical Behavior of the Dental Implant Macrodesign

Camila Lima de Andrade, DDS, MSc, PhD¹/Marco Aurélio Carvalho, DDS, MSc²/

Dimorvan Bordin, DDS, MSc²/Wander José da Silva, DDS, MSc, PhD³/

Altair Antoninha Del Bel Cury, DDS, MSc, PhD³/Bruno Salles Sotto-Maior, DDS, MSc, PhD⁴

Purpose: The aim of this study was to evaluate the influence of implant macrodesign when using different types of collar and thread designs on stress/strain distributions in a maxillary bone site. **Materials and Methods:** ~~Stress/strain values were obtained from~~ the combination of two collar designs (smooth and microthread) and three thread shapes (square, trapezoidal, and triangular) in external hexagon implants (4 × 10 mm) supporting a single zirconia crown in the maxillary first molar region. A 200-N axial occlusal load was applied to the crown, and measurements were made of the von Mises stress (σ_{VM}) for the implant, and tensile stress (σ_{max}), shear stress (τ_{max}), and strain (ϵ_{max}) for the surrounding bone using tridimensional finite element analysis. The main effects of each level of the two factors investigated (collar and thread designs) were evaluated by one-way analysis of variance (ANOVA) at a 5% significance level. **Results:** Collar design was the main factor of influence on von Mises stress in the implant and stresses/strain in the cortical bone, while thread design was the main factor of influence on stresses in the trabecular bone ($P < .05$). The optimal collar design was able to produce more favorable stress/strain distribution than the microthreaded design for the cortical bone. For the trabecular bone, the triangular thread shape had the lowest stresses and strain values among the square and trapezoidal implants. **Conclusion:** Stress/strain distribution patterns were influenced by collar design in the implant and cortical bone, and by thread design in the trabecular bone. Microthreads and triangular thread-shape designs presented improved biomechanical behavior in posterior maxillary bone when compared with the smooth collar design and trapezoidal and square-shaped threads. INT J ORAL MAXILLOFAC IMPLANTS 2017;32:xxx-xxx. doi: 10.11607/jomi.4797

[AU: Correct?]

Keywords: dental implants, finite element analysis, macrodesign, osseointegration

The predictability and long-term success rates of osseointegrated implants have been related to several factors, including material biocompatibility, implant design, surface treatment, surgical technique, micro-movement control, bone quality, and loading conditions.¹ Lower success rates for osseointegrated dental implants have been reported for maxillary implants,

especially those in the posterior maxilla, which is usually characterized by lower-density bone.² Implants that essentially have only trabecular anchorage may have a greater biomechanical challenge, due to the reduced bone-to-implant contact, poor immobilization, and lower primary stability, which can lead to micro-motion, and consequently, implant failure.³

As bone quality cannot be changed, selection of the appropriate implant design is imperative to improve the magnitude of stress that is transmitted to the bone-implant interface in the posterior maxilla in order to preserve the osseointegration.⁴ Implant design refers to three-dimensional implant structure, comprising all elements and features of the implant. The implant design may be categorized into two modalities: macrodesigns and microdesigns. Macrodesign refers to the shape of the thread, implant body, prosthetic connection, and collar design. Microdesign refers to the implant material, surface morphology, and surface treatment.⁵⁻⁷

Researchers have targeted the implant macrodesign, in attempts to understand the biomechanical factors that most affect long-term implant success during anchorage in the bone.⁸⁻²⁰ The role of the thread as the retentive element in the implant collar

¹PhD [AU: Title?], Department of Prosthodontics and Periodontology, Piracicaba Dental School, University of Campinas, Piracicaba, São Paulo, Brazil.

²PhD Student, Department of Prosthodontics and Periodontology, Piracicaba Dental School, University of Campinas, Piracicaba, São Paulo, Brazil.

³Prosthodontics Professor, Department of Prosthodontics and Periodontology, Piracicaba Dental School, University of Campinas, Piracicaba, São Paulo, Brazil.

⁴Prosthodontics Professor, Department of Restorative Dentistry, Federal University of Juiz de Fora, Juiz de Fora, Minas Gerais, Brazil.

Correspondence to: Altair Antoninha Del Bel Cury, Department of Prosthodontics and Periodontology, Piracicaba Dental School, University of Campinas, Avenida Limeira, 901, 13414-903, Piracicaba, São Paulo, Brazil. Email: altcury@fop.unicamp.br

©2017 by Quintessence Publishing Co Inc.

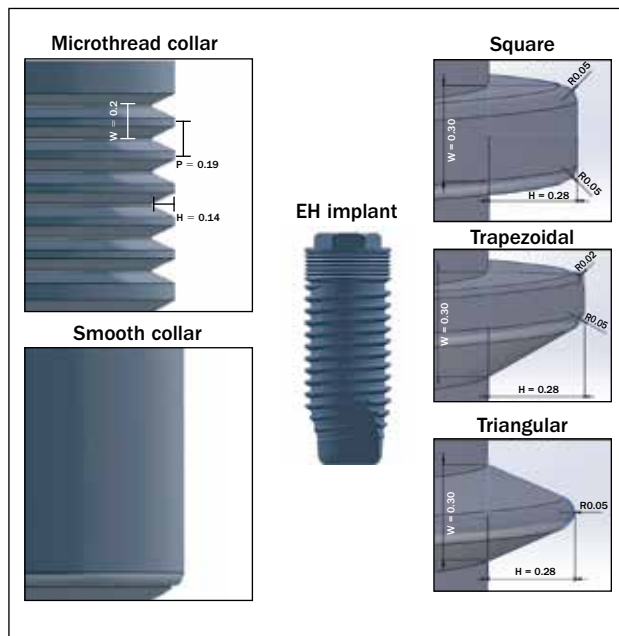


Fig 1 Schematic illustration of the collar- and thread-shape designs used in the study. Height (H), width (W), and pitch (P) of the threads are specified for the microthread collar and for different thread shapes. EH = external hexagon. [AU: Spellout correct?]

and body is related to an increased contact surface area, which provides greater bone-implant interaction and implies better stress distribution at the peri-implant bone site.^{21–26} Moreover, the thread design helps determine the maintenance of the surrounding bone and the primary stability for immediate loading conditions, especially when implants are inserted into maxillary bone.^{4,6,27,28} However, there is a lack of data in the literature about the implant macrodesign that optimizes the maintenance of osseointegrated implants anchored in sites of the maxillary posterior region and that could contribute to increasing long-term success rates. Therefore, new insights are needed to understand the biomechanical behavior of maxillary marginal bone around implants with different collar and thread designs.^{29–31}

In this context, finite element analysis (FEA) has become an increasingly powerful approach to predict the biomechanical behavior of the bone-implant interface and to identify areas of greater stress/strain concentration.^{27,32–35} Therefore, the objective of this study was to evaluate two different collar and three thread designs for single implant restorations anchored in the posterior maxilla, in terms of the stress and strain concentrations in the implant and peri-implant bone using three-dimensional (3D) FEA. In addition, this study applied statistical analysis to identify the main factors related to implant macrodesign that contribute to induce stress and strain concentrations.

MATERIALS AND METHODS

Experimental Design

With the help of computer-aided design software (SolidWorks 2014, SolidWorks Corporation), the bone models were constructed on the basis of cone-beam computed tomography cross-sectional images of an edentulous posterior human maxilla. The bone segments were 20.0 mm in buccolingual length, 11.53 mm in height, and 8.95 mm in width, with a cortical bone thickness of 1.40 mm. Cortical and trabecular bone were subdivided into peri-implant bone in direct contact with the implant and remaining bone, to isolate the region of highest interest for analysis.³⁶

Cylindrical external hexagon implants (4 mm in diameter \times 10 mm in length) were used to support cemented zirconia crowns. Implants were modeled with two types of implant collar designs (smooth collar [sm] and microthread collar [mt]) and three different implant body thread designs (square [SQ], trapezoidal [TP], and triangular [TR]), whose combination yielded six groups in total (SQsm, SQmt, TPsm, TPmt, TRsm, and TRmt). Implant models were placed vertically at the crestal bone level and constructed under similar conditions of position, height, width, and pitch thread (0.55 mm). Thread dimensions were chosen as those providing the optimal stress distribution around the osseointegrated implants, in accordance with reported studies.^{7,37,38} The collar design was obtained with a height of 1.45 mm. Collar and thread designs are specified in Fig 1.

Table 1 Mechanical Properties Assigned to the Materials Used in the Study

	Young's modulus (E) (MPa)		Shear modulus (G) (MPa)		Poisson ratio (δ)	
Cortical bone ³⁴	Ex	12,600	Gxy	4,850	δ_{xy}	0.30
	Ey	12,600	Gyz	5,700	δ_{yz}	0.39
	Ez	19,400	Gxz	5,700	δ_{xz}	0.39
Trabecular bone ^{26,34}	Ex	1,150	Gxy	6,800	δ_{xy}	0.010
	Ey	2,100	Gyz	4,340	δ_{yz}	0.32
	Ez	1,150	Gxz	6,800	δ_{xz}	0.05
Titanium (implant and abutment) ⁴⁰	104,000		38,800		0.34	
Cement ⁴¹	17,000		14,500		0.30	
Zirconia ⁹	210,000		33,000		0.31	

The subscripts x, y, and z correspond to the axis of the global coordinate system.

Table 2 Summary of ANOVA for von Mises Stress in Implant and for Tensile Stress, Shear Stress, and Strain in Cortical and Trabecular Bone

Parameters	Cortical						Trabecular							
	Implant		Tensile stress		Shear stress		Strain		Tensile stress		Shear stress		Strain	
	P	%TSS	P	%TSS	P	%TSS	P	%TSS	P	%TSS	P	%TSS	P	%TSS
Collar design	< .001	99.79	.01	96.43	< .001	99.86	.02	89.08	.69	0.27	.78	0.15	.36	6.69
Thread design	.81	0.04	.65	1.26	.19	0.11	.43	6.16	.02	97.06	.03	96.92	.10	83.44
Error		0.17		2.31		0.03		4.76		2.66		2.94		9.86
Total		100		100		100		100		100		100		100

%TSS = total sum of squares.

Numerical Analysis

All models were exported to ANSYS Workbench FEA software (version 14.0; Swanson Analysis) for mesh acquirement and numerical analysis. The mesh was generated with 0.5-mm quadratic tetrahedral elements, after convergence analysis (5%) as a refinement process to improve the accuracy of the results and guarantee the mesh quality.³⁹ Cortical and trabecular bone were assumed to be anisotropic, homogeneous, and linearly elastic. All other materials were considered to be isotropic, homogeneous, and linearly elastic. Mechanical properties of materials were determined from the literature (Table 1). The models were fully constrained in all directions at the nodes on the mesial and distal borders. A 200-N occlusal load was distributed in five 1.5-mm² contact areas on the occlusal surface of the crown.

Statistical Analysis

Using 3D FEA, quantitative analysis was performed according to the von Mises (σ_{VM}) criterion for the implant, and the tensile stress (σ_{max}), shear stress (τ_{max}), and strain (ϵ_{max}) for the cortical and trabecular bone.⁴² Data were analyzed qualitatively according to the stress distribution patterns in the implant and the cortical and trabecular bone. All combinations of the implant collar designs and implant-body thread shapes

were considered (SQsm, SQmt, TPsm, TPmt, TRsm, and TRmt), resulting in six calculation sets. Data from each level of the two investigated factors (collar design and thread shape) were evaluated based on statistical methods using SAS (SAS version 9.0; SAS Institute) for analysis of variance (ANOVA). This analysis allowed the authors to calculate the percentage of the contribution (% total sum of squares) of each investigated factor. The significance level was set at 5%.⁴³

RESULTS

Stress Distribution in the Implant

Collar design significantly affected the von Mises stress in the implant ($P < .001$), determining the magnitude of the stress and contributing 99.79% of the total generated stress. Thread design did not significantly influence the von Mises stress (contribution < 1%, $P > .05$, Table 2). A lower peak of stress was noted in the [sm] groups compared with the [mt] groups (Table 3). Stress was concentrated in the implant cervical area for both collar designs. Maximal stress appeared at the palatal side, under the flank of the first microthread (Fig 2). The stress distribution pattern differed between collar designs. Stress in all the [sm] groups decreased in the apical direction, with a gradual curving pattern,

Table 3 Maximum von Mises Stress (MPa) in Implants and the Peak Maximum of Tensile Stress (MPa), Shear Stress (MPa), and Strain ($E10^{-4} \mu\text{m}$) in Cortical and Trabecular Bone Around Different Implant Designs

Implant designs	Maximum von Mises (MPa)	Cortical bone			Trabecular bone		
		Tensile stress (MPa)	Shear stress (MPa)	Strain (μm)	Tensile stress (MPa)	Shear stress (MPa)	Strain (μm)
SQsm	23.74	10.98	9.51	7.34	6.34	6.52	8.69
TPsm	23.79	11.27	9.53	7.38	7.68	8.25	11.87
TRsm	24.85	11.24	9.56	7.43	3.59	3.81	8.72
SQmt	56.10	9.23	11.93	9.11	5.73	5.79	10.38
TPmt	54.54	9.27	11.95	9.55	8.35	8.73	11.59
TRmt	54.09	8.72	12.06	10.49	4.07	4.47	9.31

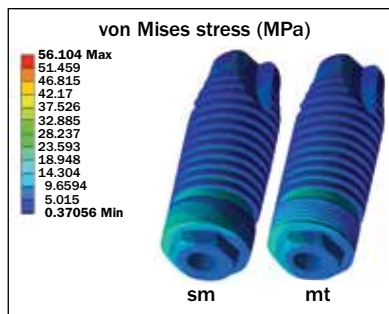


Fig 2 Concentration of von Mises stress (MPa) in the implant for different collar designs. sm = smooth collar; mt = microthread collar.

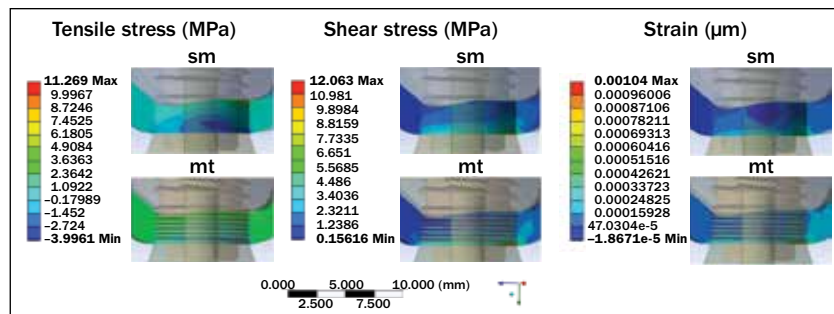


Fig 3 Distribution of tensile stress (MPa), shear stress (MPa), and strain (μm) in the cortical bone with the smooth collar (sm) and microthread collar (mt) designs.

whereas stress in the [mt] groups had a wavy pattern along the implant neck (Fig 2).

Stress/Strain Distributions in Cortical Bone

When focusing on the cortical bone area, collar design not only significantly affected tensile ($P = .01$) and shear ($P = .001$) stresses, but also influenced strain ($P = .02$), with contributions of 96.43%, 99.86%, and 89.08% of the total generated tensile stress, shear stress, and strain, respectively. Thread design did not affect cortical bone (Table 2). Maximal tensile stress was observed for the [sm] groups, whereas maximal shear stress and strain were noted for the [mt] groups (Table 3).

The stress/strain distribution pattern in cortical bone differed between collar designs (Fig 3). The [mt] groups exhibited a uniform tensile stress concentration around the cortical bone, whereas the shear stress and strain distributions had heterogeneous patterns. Shear stress and strain concentrations were higher at the thread crest and lower at the thread base, creating a wavy pattern downward along the interface. Tensile stress in the [sm] groups exhibited a U-shaped pattern, whereas the shear stress and strain created uneven curves around the cortical bone.

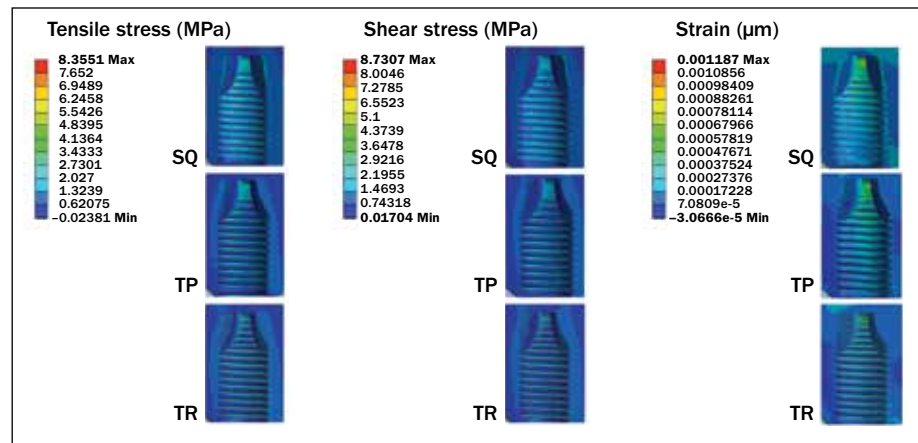
Stress/Strain Distributions in Trabecular Bone

In trabecular bone, the thread design significantly influenced tensile and shear stresses ($P < .05$), but the collar design had no influence. Thread design contributed 97.06% and 96.92% of the total generated tensile and shear stresses, respectively (Table 2). The TR thread shape produced lower tensile stress, shear stress, and strain than the SQ and TP thread shapes, for which the stresses were twice those of TR (Table 3). Stress and strain were observed in the areas surrounding the threads in the middle and apex of the implant. For all thread designs, the lowest stress values were observed at the bottom of the threads, represented by the thread base (Fig 4).

DISCUSSION

Several studies have investigated implant macrodesign, attempting to minimize crestal bone resorption and osseointegration loss after restoration by improving the stress/strain distribution at the marginal crest and in peri-implant bone.^{1,11,24,33-35} To enhance the clinical success of maxillary implants, it is necessary to understand how the biomechanical behaviors of the

Fig 4 Distribution of tensile stress (MPa), shear stress (MPa), and strain (μm) in trabecular bone for threads with square (SQ), trapezoidal (TP), and triangular (TR) shapes.



implant and supporting bone are affected by different collar and thread designs, as well as to determine which parameters most contribute to the generated stress and strain. The present study used FEA with statistical analysis to interpret the biomechanical behavior of implants with different macrodesigns and to evaluate the main factors of influence on stress/strain concentration in low-quality bone.

In this study, the von Mises (σ_{VM}) criterion was used for the implant, as it is an adequate stress criterion to evaluate the behavior of ductile materials such as titanium. The tensile stress (σ_{max}), shear stress (τ_{max}), and strain (ϵ_{max}) criteria for the cortical and trabecular bone were used to establish the stress behavior in brittle materials such as bone tissue.³⁹

Collar design was the main factor of influence on von Mises stress in the implants. The highest stress value was observed with the [mt] implants, and the stress distribution was characterized by a wavy pattern along the microthreads at the palatal side. Higher stress concentration was seen in the flank of the microthreads, and lower stress was localized on top of them. The discontinuity of the microthreads could have been the main factor in this stress distribution pattern.²³ In the [sm] implants, the stress decreased from top to bottom of the collar region, exhibiting a curved pattern. This decreasing stress was likely influenced by the decreasing functional surface area of the smooth collar present in the implant, which would have led to the dissipation of stress at the cervical region.^{10,19}

Similarly as in the implants, collar design was the main factor of effect on stresses and strain in cortical bone. When tensile stress was evaluated in the cortical bone, the [sm] groups presented a higher peak of stress when compared with the [mt] groups. It was concentrated in a small apical area of the cortical bone, although tensile stress was distributed throughout all of the cortical bone with values below 1.1 MPa (Fig 4). The literature reports that 1.6 MPa of stress is needed to

prevent disuse bone atrophy in cortical bone.^{10,16,20,33} Therefore, bone loss around the smooth collar may be a consequence of disuse atrophy, due to subnormal mechanical stimulation of the bone in accordance with Wolff's Law.^{10,20} However, bone loss can also occur by overloading of the cortical bone, in which the physical limit of bone strength is exceeded due to the highest values of stress at the cortical bone. **[AU: Correct?]** The ultimate bone strength can be assumed to represent the physiologic limit. Thus, overloading of cortical bone tissue can lead to bone resorption and can be detected when tensile stress exceeds 100 to 130 MPa.^{44,45}

Clinical findings have confirmed that initial bone loss around a smooth collar implant coincides with exposure of the implant to the intraoral environment in stage two of surgery or after loading, and that the resorption pattern is V- or U-shaped (referred to as "saucerization").³¹ In the present study, the tensile stress distribution around the [sm] groups formed a U-shaped pattern, compatible with the crestal bone loss reported in the literature.^{5,31} In contrast, for the [mt] groups, the magnitude of the tensile stress exceeded 1.6 MPa. Moreover, the tensile stress was concentrated uniformly around the cortical bone, exerting an optimal effect for stress distribution and maintaining the peri-implant marginal bone level.^{15,33}

In cortical bone, greater magnitudes of shear stress and strain were observed with the [mt] implants compared with the [sm] implants. The effects of the microthreads as retentive elements can explain the increase of stress/strain in cortical bone.²³ Stress and strain tended to be more concentrated at the thread crest, whereas their magnitudes were decreased at the thread base, creating a heterogeneous stress/strain distribution pattern. The microthread-induced stress concentration in the cortical bone was analogous to the stress concentration in the implant. Specifically, when shear stress was higher in the microthread flank

in the implant, it was lower in the cortical bone in the same area, whereas when shear stress was lower on the microthread crest, it was higher in the cortical bone. Hence, microthreads can control stress/strain transference from the implant to the cortical bone.

Moreover, microthreads at the implant neck can mechanically stimulate cortical bone, maintaining an appropriate level of stimulus.^{10,27} Nonphysiologic levels of stress may stimulate osteoclastic activities, resulting in microdamage and bone resorption.^{11,19,20,32} In contrast, the smooth collar does not provide sufficient stimulus to preserve the cortical bone.²⁰ The high stress concentrations at the thread crest induced by microthreads were considered to have a positive effect on the cortical bone, because moderate stress/strain levels were maintained. The mechanical stress theory states that mild overload at the thread crest triggers osteoblasts to initiate bone formation in the stressed area. Indeed, active bone formation at the thread crest has been demonstrated in experimental studies.^{8,18,28} This theory is also consistent with clinical studies, which have shown that microthreads reduce cortical bone loss and stabilize the osseointegration process.^{11,15,17}

The findings of this study showed that the thread design was the main factor of influence on tensile and shear stresses in trabecular bone, contributing more than 95% of the total stress. The SQ and TP thread shapes presented twice as much stress/strain as the TR thread shape. The literature reports that local overloading at the trabecular bone occurs when tensile stress exceeds 5 MPa.^{44,45} The unique thread implant design that did not exceed the tolerance limit was the TR thread shape. The lower stress levels produced by the TR thread shape can be explained by its smaller flank angle at the bottom of the thread.^{19,32} Lower stresses in trabecular bone reportedly can improve osseointegration and enhance bone-to-implant contact.⁴⁶ In trabecular bone, the stress/strain was localized at the top of the threads and apex of the implant, with lower concentrations at the thread base. Compared with other thread designs, the TR thread shape not only showed lower stresses near the top of the thread, but also a greater area of low stress on the thread base in contact with trabecular bone. Thus, this thread shape may be more appropriate for stress/strain dissipation in posterior maxillary bone sites. Overall, the thread morphology played an important role in the stress concentration at the implant-bone interface.^{17,19,32,38}

This study analyzed only a bonded bone-implant interface and axial loading. Studies have demonstrated that nonbonded contact surfaces and oblique loading influence stress/strain patterns in bone near the interface, producing doubled stresses and strains compared with a bonded interface and axial loading.^{9,24,26}

The effects of a nonbonded interface and oblique loading in the posterior maxilla need to be investigated.

From a biomechanical perspective, both the collar and thread designs are important factors affecting stress/strain in the surrounding tissue and implant osseointegration. The [mt] can be suggested for the maintenance of cortical crestal bone. The TR thread shape showed the ability to decrease the stress concentration and better dissipate bone stresses in trabecular bone.

CONCLUSIONS

When compared with a smooth collar, a microthread design positively influenced the biomechanical behavior of a single implant restoration anchored in posterior maxillary bone. Likewise, a triangular thread design results in lower stress when compared with square- or trapezoidal-shaped threads in a simulated bounded bone-to-implant contact surface.

ACKNOWLEDGMENTS

The authors reported no conflicts of interest related to this study. [AU: Okay?]

REFERENCES

1. Amid R, Raoofi S, Kadkhodazadeh M, Movahhedi MR, Khademi M. Effect of microthread design of dental implants on stress and strain patterns: A three-dimensional finite element analysis. *Biomed Tech (Berl)* 2013;58:457–467.
2. Jaffin RA, Berman CL. The excessive loss of Brånemark fixtures in type IV bone: A 5-year analysis. *J Periodontol* 1991;62:2–4.
3. Orsini E, Giavaresi G, Trirè A, Ottani V, Salgarello S. Dental implant thread pitch and its influence on the osseointegration process: An in vivo comparison study. *Int J Oral Maxillofac Implants* 2012;27:383–392.
4. Hermann F, Lerner H, Palti A. Factors influencing the preservation of the periimplant marginal bone. *Implant Dent* 2007;16:165–175.
5. Steigenga JT, al-Shammari KF, Nociti FH, Misch CE, Wang HL. Dental implant design and its relationship to long-term implant success. *Implant Dent* 2003;12:306–317.
6. Abuhussein H, Pagni G, Rebaudi A, Wang HL. The effect of thread pattern upon implant osseointegration. *Clin Oral Implants Res* 2010;21:129–136.
7. Geng JP, Xu DW, Tan KB, Liu GR. Finite element analysis of an osseointegrated stepped screw dental implant. *J Oral Implantol* 2004;30:223–233.
8. Negri B, Calvo Guirado JL, Maté Sánchez de Val JE, Delgado Ruíz RA, Ramírez Fernández MP, Barona Dorado C. Peri-implant tissue reactions to immediate nonocclusal loaded implants with different collar design: An experimental study in dogs. *Clin Oral Implants Res* 2014;25:54–63.
9. Fuh LJ, Hsu JT, Huang HL, Chen MY, Shen YW. Biomechanical investigation of thread designs and interface conditions of zirconia and titanium dental implants with bone: Three-dimensional numeric analysis. *Int J Oral Maxillofac Implants* 2013;28:64–71.
10. Choi KS, Park SH, Lee JH, Jeon YC, Yun MJ, Jeong CM. Stress distribution on scalloped implants with different microthread and connection configurations using three-dimensional finite element analysis. *Int J Oral Maxillofac Implants* 2012;27:29–38.

11. Kang YI, Lee DW, Park KH, Moon IS. Effect of thread size on the implant neck area: Preliminary results at 1 year of function. *Clin Oral Implants Res* 2012;23:1147–1151.
12. Rismanchian M, Birang R, Shahmoradi M, Talebi H, Zare RJ. Developing a new dental implant design and comparing its biomechanical features with four designs. *Dent Res J* 2010;7:70–75.
13. Limbert G, van Lierde C, Muraru OL, et al. Trabecular bone strains around a dental implant and associated micromotions—A micro-CT-based three-dimensional finite element study. *J Biomech* 2010;43:1251–1261.
14. Lee CC, Lin SC, Kang MJ, Wu SW, Fu PY. Effects of implant threads on the contact area and stress distribution of marginal bone. *J Dent Sci* 2010;5:156–165.
15. Song DW, Lee DW, Kim CK, Park KH, Moon IS. Comparative analysis of peri-implant marginal bone loss based on microthread location: A 1-year prospective study after loading. *J Periodontol* 2009;80:1937–1944.
16. Schrottenboer J, Tsao YP, Kinariwala V, Wang HL. Effect of microthreads and platform switching on crestal bone stress levels: A finite element analysis. *J Periodontol* 2008;79:2166–2172.
17. Lee DW, Choi YS, Park KH, Kim CS, Moon IS. Effect of microthread on the maintenance of marginal bone level: A 3-year prospective study. *Clin Oral Implants Res* 2007;18:465–470.
18. Abrahamsson I, Berglund T. Tissue characteristics at microthreaded implants: An experimental study in dogs. *Clin Implant Dent Relat Res* 2006;8:107–113.
19. Hansson S, Werke M. The implant thread as a retention element in cortical bone: The effect of thread size and thread profile: A finite element study. *J Biomech* 2003;36:1247–1258.
20. Hansson S. The implant neck: Smooth or provided with retention elements. A biomechanical approach. *Clin Oral Implants Res* 1999;10:394–405.
21. Desai SR, Desai MS, Katti G, Karthikeyan I. Evaluation of design parameters of eight dental implant designs: A two-dimensional finite element analysis. *Niger J Clin Pract* 2012;15:176–181.
22. Aparna IN, Dhanasekar B, Lingeshwar D, Gupta L. Implant crest module: A review of biomechanical considerations. *Indian J Dent Res* 2012;23:257–263.
23. Meriç G, Erkmén E, Kurt A, Eser A, Ozden AU. Biomechanical comparison of two different collar structured implants supporting 3-unit fixed partial denture: A 3-D FEM study. *Acta Odontol Scand* 2012;70:61–71.
24. Hudieb MI, Wakabayashi N, Kasugai S. Magnitude and direction of mechanical stress at the osseointegrated interface of the microthread implant. *J Periodontol* 2011;82:1061–1070.
25. Eraslan O, Inan O. The effect of thread design on stress distribution in a solid screw implant: A 3D finite element analysis. *Clin Oral Investig* 2010;14:411–416.
26. Huang HL, Chang CH, Hsu JT, Fallgatter AM, Ko CC. Comparison of implant body designs and threaded designs of dental implants: A 3-dimensional finite element analysis. *Int J Oral Maxillofac Implants* 2007;22:551–562.
27. Vidyasagar L, Apse P. Dental implant design and biological effects on bone-implant interface. *Balt Dent Maxillofac J* 2004;6:51–54.
28. Chowdhary R, Halldin A, Jimbo R, Wennerberg A. Influence of microthreads alteration on osseointegration and primary stability of implants: An FEA and in vivo analysis in rabbits. *Clin Implant Dent Relat Res* 2013;1–8.
29. Sevımay M, Turhan F, Kiliçarslan MA, Eskitascioğlu G. Three-dimensional finite element analysis of the effect of different bone quality on stress distribution in an implant-supported crown. *J Prosthet Dent* 2005;93:227–234.
30. Tada S, Stegaroiu R, Kitamura E, Miyakawa O, Kusakari H. Influence of implant design and bone quality on stress/strain distribution in bone around implants: A 3-dimensional finite element analysis. *Int J Oral Maxillofac Implants* 2003;18:357–368.
31. Misch CE. Implant design considerations for the posterior regions of the mouth. *Implant Dent* 1999;8:376–386.
32. Chowdhary R, Halldin A, Jimbo R, Wennerberg A. Evaluation of stress pattern generated through various thread designs of dental implants loaded in a condition of immediately after placement and on osseointegration—an FEA study. *Implant Dent* 2013;22:91–96. **[Unconfirmed]**
33. Khurana P, Sharma A, Sodhi KK. Influence of fine threads and platform-switching on crestal bone stress around implant—a three-dimensional finite element analysis. *J Oral Implantol* 2013;39:697–703.
34. Lan TH, Du JK, Pan CY, Lee HE, Chung WH. Biomechanical analysis of alveolar bone stress around implants with different thread designs and pitches in the mandibular molar area. *Clin Oral Investig* 2012;16:363–369.
35. Atieh MA, Shahmiri RA. Evaluation of optimal taper of immediately loaded wide-diameter implants: A finite element analysis. *J Oral Implantol* 2013;39:123–132.
36. De Cos Juez FJ, Sánchez Lasheras F, García Nieto PJ, Álvarez-Arenal A. Non-linear numerical analysis of a double-threaded titanium alloy dental implant by FEM. *Appl Math Comput* 2008;206:952–967.
37. Kong L, Hu K, Li D, et al. Evaluation of the cylinder implant thread height and width: A 3-dimensional finite element analysis. *Int J Oral Maxillofac Implants* 2008;23:65–74.
38. Chun HJ, Cheong SY, Han JH, et al. Evaluation of design parameters of osseointegrated dental implants using finite element analysis. *J Oral Rehabil* 2002;29:565–574.
39. Sotito-Maior BS, Senna PM, da Silva WJ, Rocha EP, Del Bel Cury AA. Influence of crown-to-implant ratio, retention system, restorative material, and occlusal loading on stress concentrations in single short implants. *Int J Oral Maxillofac Implants* 2012;27:13–18.
40. Sotito-Maior BS, Rocha EP, de Almeida EO, Freitas-Júnior AC, Anchieta RB, Del Bel Cury AA. Influence of high insertion torque on implant placement: An anisotropic bone stress analysis. *Braz Dent J* 2010;21:508–514.
41. Li L, Wang Z, Bai ZC, et al. Three-dimensional finite element analysis of weakened roots restored with different cements in combination with titanium alloy posts. *Chin Med J* 2006;119:305–311.
42. Dejak B, Mlotkowski A. Three-dimensional finite element analysis of strength and adhesion of composite resin versus ceramic inlays in molars. *J Prosthet Dent* 2008;99:131–140.
43. Dar FH, Meakin JR, Aspden RM. Statistical methods in finite element analysis. *J Biomech* 2002;35:1155–1161.
44. Martin RB, Burr DB, Sharkey NA. *Skeletal Tissue Mechanics*. New York: Springer, 1998:127–178.
45. Baggi L, Cappelloni I, Di Girolamo M, Maceri F, Vairo G. The influence of implant diameter and length on stress distribution of osseointegrated implants related to crestal bone geometry: A three-dimensional finite element analysis. *J Prosthet Dent* 2008;100:422–431.
46. Limbert G, van Lierde C, Muraru OL, et al. Trabecular bone strains around a dental implant and associated micromotions—A micro-CT-based three-dimensional finite element study. *J Biomech* 2010;43:1251–1261.